# *Drivers of recent North Pacific decadal variability: the role of aerosol forcing*



Dittus, A. J. ORCID: https://orcid.org/0000-0001-9598-6869, Hawkins, E. ORCID: https://orcid.org/0000-0001-9477-3677, Robson, J. I. ORCID: https://orcid.org/0000-0002-3467-018X, Smith, D. M. and Wilcox, L. J. ORCID: https://orcid.org/0000-0001-5691-1493 (2021) Drivers of recent North Pacific decadal variability: the role of aerosol forcing. Earth's Future, 9 (12). e2021EF002249. ISSN 2328-4277 doi: https://doi.org/10.1029/2021EF002249 Available at https://centaur.reading.ac.uk/101162/

Earth's Future

RESEARCH ARTICLE
10.1029/2021EF002249

# Drivers of Recent North Pacific Decadal Variability: The Role of Aerosol Forcing

**Andrea J. Dittus[1], Ed Hawkins[1], Jon I. Robson[1], Doug M. Smith[2], and Laura J. Wilcox[1]**

[1]National Centre for Atmospheric Science and Department of Meteorology, University of Reading, Reading, UK, [2]Met Office Hadley Centre, Exeter, UK

**Key Points:**

- Anthropogenic aerosols can induce an increase in North Pacific sea level pressure in GCMs and promote a negative Pacific Decadal Oscillation over 1981–2012
- This circulation-mediated Pacific cooling in response to anthropogenic aerosol is weaker than GHG-induced warming
- GCMs appear unable to capture the strength of the observed cooling in the Pacific during this period and possible causes are discussed

**Supporting Information:**

Supporting Information may be found in the online version of this article.

**Correspondence to:**

A. J. Dittus,
a.j.dittus@reading.ac.uk

**Citation:**

Dittus, A. J., Hawkins, E., Robson, J. I., Smith, D. M., & Wilcox, L. J. (2021). Drivers of recent North Pacific Decadal Variability: The role of aerosol forcing. *Earth's Future*, *9*, e2021EF002249. https://doi.org/10.1029/2021EF002249

Received 7 JUN 2021
Accepted 5 NOV 2021



**Abstract** Climate variability in the Pacific has an important influence on climate around the globe. In the period from 1981 to 2012, there was an observed large-scale cooling in the Pacific. This cooling projected onto the negative phase of the Pacific Decadal Oscillation (PDO) and contributed to a slowdown in the rate of near-surface temperature warming. However, this cooling pattern is not simulated well by the majority of coupled climate models and its cause is uncertain. We use large multi-model ensembles from the sixth Climate Model Intercomparison Project, and an ensemble of simulations with HadGEM3-GC3.1-LL that is specifically designed to sample the range of uncertainty in historical anthropogenic aerosol forcing, to revisit the role of external forcings. We show that anthropogenic aerosols can drive an atmospheric circulation response via an increase in North Pacific sea level pressure and contribute to a negative PDO during this period in several global climate models. In HadGEM3, this increase in North Pacific sea-level pressure is associated with an anomalous Rossby Wave train across the North Pacific, which is also seen in observations. Our results provide further evidence that anthropogenic aerosols may have contributed to observed cooling in the Pacific in this period. However, the simulated cooling in response to aerosol forcing is substantially weaker than the warming induced by greenhouse gases, resulting in simulations that are warming faster than observations, and further highlighting the need to understand whether models correctly simulate atmospheric circulation responses.

**Plain Language Summary** Climate variability in the Pacific has an important influence on climate around the globe. In the period from 1981 to 2012, there was an observed large-scale cooling in the Pacific. The causes of this observed cooling are still uncertain. Climate models are able to simulate similar cooling patterns, but these are often weaker than observed. We show that anthropogenic aerosols, tiny particles emitted by human activity, have likely contributed to observed cooling in the Pacific since the 1980s via changes in atmospheric circulation. The simulated response to anthropogenic aerosols is weaker than the warming response to greenhouse gases, resulting in a majority of climate model simulations that are warming faster than observations over this period. We speculate that Pacific cooling induced by atmospheric circulation changes in response to aerosol may be underestimated in current global climate models, but other hypotheses exist, highlighting the need for further research in this area.

## 1. Introduction

Understanding what drives multi-decadal variations in the Pacific has been a topic of research for many decades. Pacific sea surface temperatures (SSTs) are an important contributor to setting the rate of warming in global mean surface temperatures (e.g., Kajtar et al., 2019; Meehl et al., 2016). Teleconnections from the Pacific make Pacific climate variability important for many regions of the globe. The most prominent mode of interannual climate variability, the El Niño Southern Oscillation, is hugely important for climate across the world (e.g., McPhaden et al., 2006). On longer timescales, the Pacific Decadal Oscillation (PDO) or Interdecadal PDO and their drivers have been widely studied (e.g., Mantua and Hare, 2002; Schneider & Cornuelle, 2005; Newman et al., 2016; Power et al., 1999) and shown to modulate climate variability in many regions of the world (e.g., Barnett et al., 1999; Dong and Dai, 2015; Salinger et al., 2001; Wang et al., 2008; Zanchettin et al., 2008).

In recent years, significant attention has been devoted to understanding the so-called "global warming hiatus" over the period from 1998 to 2012 and the role of Pacific SSTs in explaining slower warming during that period (England et al., 2014; Kosaka & Xie, 2013; Maher et al., 2014; Medhaug et al., 2017; Meehl et al., 2013; Xie & Kosaka, 2017), though estimates of the importance of the Pacific for global temperatures vary across studies (Stolpe et al., 2020). Nevertheless, it seems clear that the Pacific has played an important role in setting the rate

of GMST increase over this period. It is less clear, however, how external forcings have affected Pacific Decadal Variability during that time. Recent studies have found roles for volcanic and anthropogenic aerosols contributing to SST variability in all ocean basins over the historical period, including the Pacific (Deser et al., 2020; Liguori et al., 2020; Qin et al., 2020). Anthropogenic aerosols (among other forcing agents such as volcanic eruptions) have previously been proposed as a driver of North Pacific SSTs (Boo et al., 2015; Smith et al., 2016). They have also been implicated for contributing to SST variability in the Pacific over the recent hiatus period (Smith et al., 2016), but other studies have found no role for anthropogenic aerosols on early 21st century temperature trends (Oudar et al., 2018).

Robustly quantifying the role of aerosols for recent Pacific Decadal Variability is difficult for several reasons. First, the magnitude of historical aerosol forcing itself is highly uncertain (Bellouin et al., 2020), and given the same emissions, different climate models will generate a wide range of historical aerosol forcing due to large diversity in aerosol schemes and their representation of aerosol processes (e.g., Wilcox et al., 2015). Beyond uncertainty in aerosol forcing and model diversity, small ensemble sizes in the presence of large internal variability and biases in the representation of processes important for Pacific climate variability (e.g., McGregor et al., 2018) render a robust quantification of the role of aerosol forcing for recent trends in Pacific temperatures difficult.

Nevertheless, understanding what drives observed variability in the Pacific is crucially important, especially in light of new challenges in the interpretation of climate projections from several climate models with high climate sensitivities in the most recent iteration of the Coupled Model Intercomparison Project (CMIP6, Eyring et al., 2016). Many of these models have warming trends inconsistent with observations since the 1980s, and it has been argued that this recent period can be used to constrain future climate projections (e.g., Brunner et al., 2020), but this approach relies on the assumption that models can simulate the effects of anthropogenic aerosols and volcanic eruptions accurately. Some of this rapid warming in climate models stems from the fact that Pacific SSTs are warming substantially faster than observations during this period (e.g., Olonscheck et al., 2020). Therefore, understanding the drivers of real-world Pacific SST variability is necessary in the context of interpreting this period of rapid warming in global climate models. It is therefore timely to reexamine the evidence for aerosol forcing contributing to historical Pacific SST variability in the most recent generation of climate models and in observations. Additionally, reductions in aerosol emissions across the globe in coming decades are likely to be important for regional climate change. It is therefore important to understand the implications of reducing aerosol burden for climate variability in the Pacific.

Here, we use CMIP6 data and a large ensemble of historical simulations with the HadGEM3-GC3.1-LL model to investigate the role of aerosol forcing for North Pacific climate variability since the 1980s. The HadGEM3 ensemble, known as the SMURPHS ensemble (Dittus et al., 2020), was run with varying levels of anthropogenic aerosol and precursor emissions across the ensemble, thus allowing the identification of responses to changes in anthropogenic aerosols. We assess the evidence for a role of anthropogenic aerosol forcing in explaining historical Pacific SSTs in CMIP6 and investigate the mechanisms responsible in the HadGEM3 global climate model. Existing hypotheses and remaining questions in reconciling observed and simulated Pacific temperature trends since the 1980s are discussed.

## 2. Data and Methods

Several types of simulations are used in this paper. First, simulations from the CMIP6 historical experiments are used to compare with observations, while simulations from the Detection and Attribution experiments (DAMIP, Gillett et al. (2016)) are used to identify which forcing agents are responsible for the forced response in the historical experiments. The DAMIP simulations are single-forcing experiments, where one forcing of interest is changing through time, and all other forcings are kept at constant pre-industrial levels. The experiments used in this paper are historical (all forcings), hist-aer (aerosol-only), hist-GHG (greenhouse gases only), and hist-nat (natural forcings only, i.e., solar and volcanic). We use all simulations available at the time of writing. The number of ensemble members available for each model varies with the experiment and variable considered, so we have chosen to use all ensemble members available for a given experiment, regardless of whether the same ensemble members are also available for other variables and experiments. As such, the number of members can vary from one experiment to the next. Note that multi-model averages are constructed from each model's ensemble mean, where all models with >= 3 ensemble members are considered. The CanESM5 contribution is

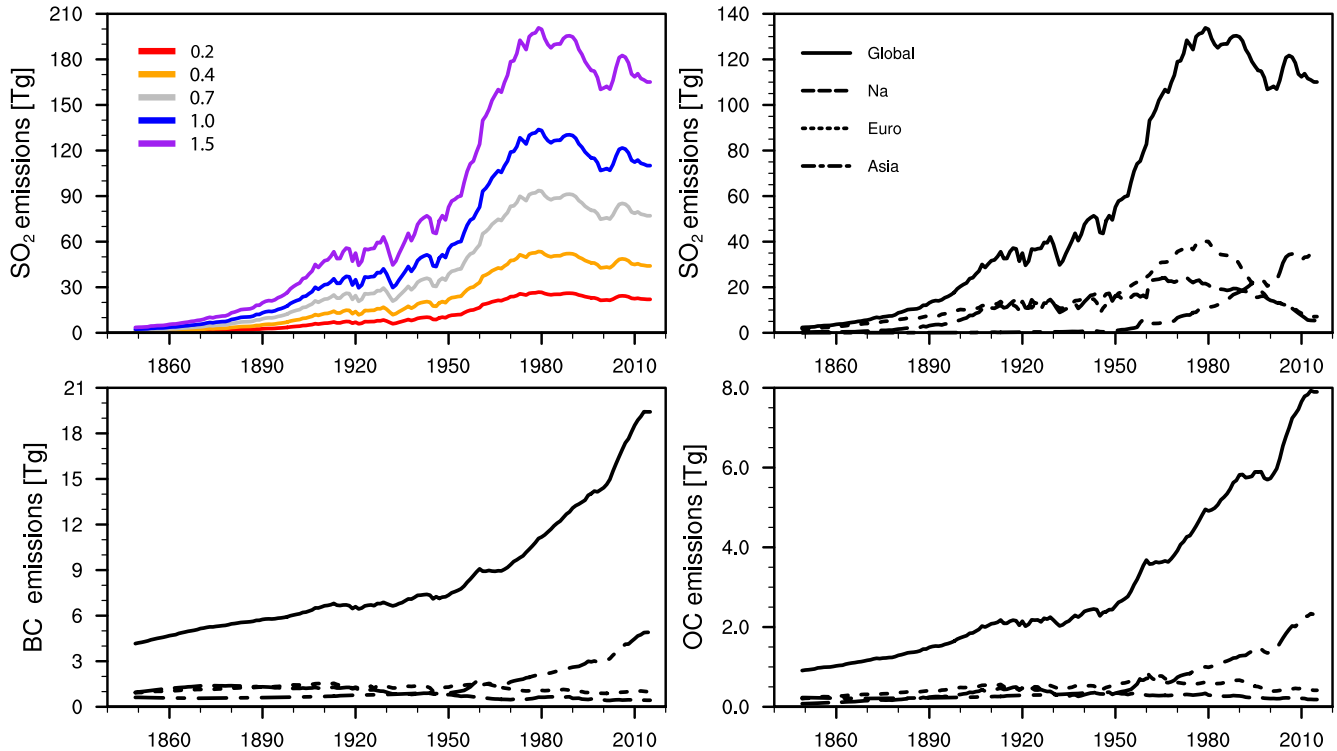


**Figure 1.** (a) Globally averaged scaled $SO_2$ emission time series, as an illustration for how the scaling factors were applied to the emission time series [the same were applied to organic carbon (OC) and black carbon (BC)]. b) $SO_2$ emissions for the 1.0 scaling, split into Global, North American, European, and Asian emissions. Panels (c) and (d) show the same for BC and OC, respectively.

also shown separately to the CMIP6 multi-model ensemble, as this modeling center provides a large ensemble size for all experiments, including the single-forcing experiments. There are 50 ensemble members available for this model for the historical, hist-GHG, and hist-nat experiments, and 30 for the hist-aer experiments (Swart et al., 2019). All the CMIP6 models used and the number of ensemble members per experiment are listed in Table S1 in Supporting Information S1.

Second, the SMURPHS ensemble is used to investigate the mechanisms associated with aerosol forcing in more detail. This ensemble consists of historical simulations with the HadGEM3-GC3.1-LL climate model, where anthropogenic aerosol emissions have been scaled by five factors (0.2, 0.4, 0.7, 1.0, and 1.5) to sample the wide uncertainty range in historical aerosol forcing (Dittus et al., 2020). These scaling factors have been applied to anthropogenic aerosol and precursor emissions (black and organic carbon and sulfur dioxide) from 1850, as illustrated for $SO_2$ in Figure 1a. Biomass burning emissions were not scaled in this experiment design. The resulting aerosol effective radiative forcings (ERF) for the year 2014 are −0.38, −0.60, −0.93, −1.17, and −1.50 W/m$^2$, respectively. Five initial condition members have been run for each of these aerosol scaling experiments, resulting in an ensemble of 25 historical simulations in total (5 × 5). The version of HadGEM3 used in this ensemble corresponds to a pre-release of the HadGEM3 model used for the CMIP6 simulations and differs from the CMIP6 version only in its treatment of ozone. More detail can be found in the Supplementary Information of Dittus et al. (2020) and Hardiman et al. (2019). The 1.0 scaling simulations are equivalent to the historical simulations documented in Andrews et al. (2020) but are separate model integrations, noting the difference in the model version described above.

The observational data sets used in this study are the ensemble mean of the HadCRUT5 analysis for near-surface temperatures (Morice et al., 2021) and HadSLP2 for sea level pressure data (Allan & Ansell, 2006). The variance-adjusted data set was used for the HadSLP2 data set from 2005 to 2012. For meridional winds at 250 hPa, we compare the SMURPHS simulations to data from the ERA5 reanalysis (Hersbach et al., 2019).

To calculate multi-model quantities, the CMIP6 simulations were regridded to a common resolution of 2.5° × 2.5° using bilinear interpolation. Where pattern correlations between observations and model simulations

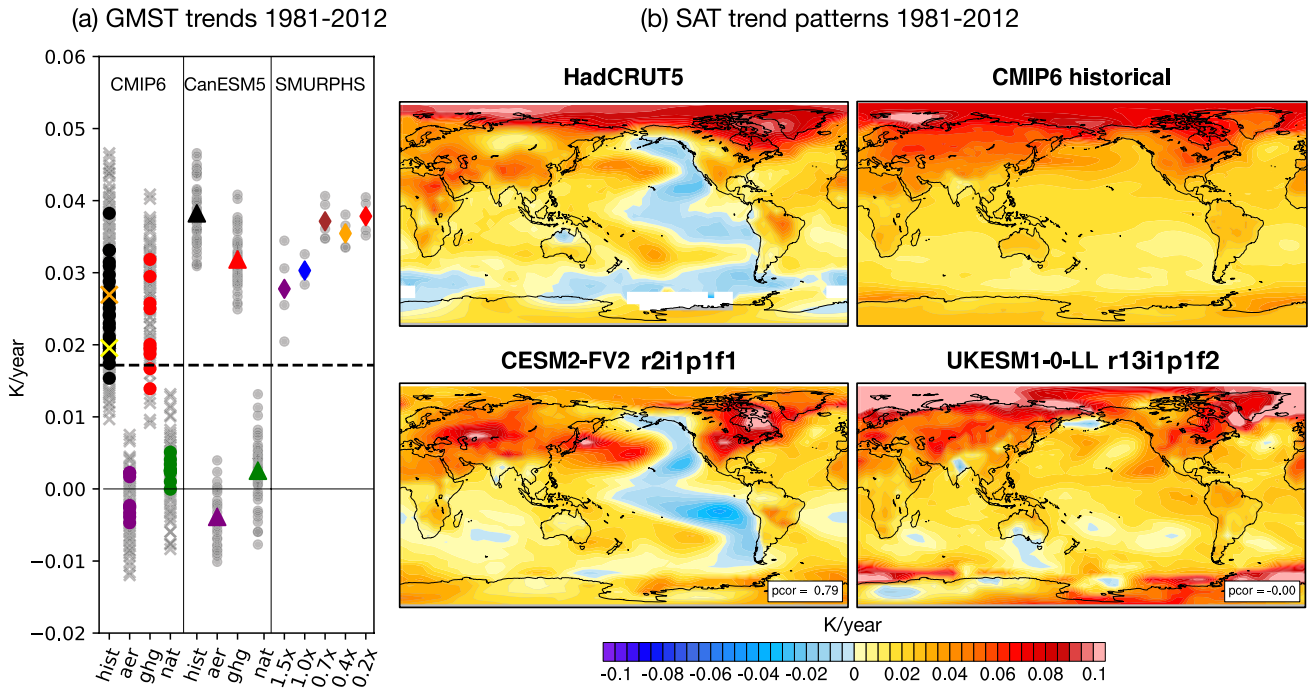


**Figure 2.** (a) Trends in annual mean GMST in the CMIP6 historical, hist-aer, hist-GHG, and hist-nat experiments, respectively, for 1981–2012. Solid dots indicate ensemble means for each model with more than three ensemble members, gray crosses represent each individual ensemble member. The same is also shown for the CanESM5 large ensemble separately (50, 30, 50, and 50 ensemble members, respectively, triangles show the ensemble mean). The dashed horizontal line shows the observed trend from HadCRUT5 over this period. b) Patterns of SAT trends in HadCRUT5, the CMIP6 ensemble mean, as well as two individual ensemble members, corresponding to the ensemble member with the highest pattern correlation with observations in the Pacific region between (CESM2-FV2) and the ensemble member with a pattern correlation in the Pacific closest to 0 (UKESM1-0-LL). These members are shown to illustrate the range of patterns seen across CMIP6 due to internal variability. The pattern correlations were calculated between −50 to 50°N and 90 to 270°E. These ensemble members are shown by yellow and orange crosses in a) respectively.

were calculated, the simulations were regridded to the resolution of the observational data set for HadCRUT5 and HadSLP2, while for Figure 7 ERA5 was regridded to the resolution of the model simulations (regridding to the lowest resolution in all cases). To calculate SLP trends over the North Pacific, area averages were computed over a box from 30° to 65° N and 160°–220° E, using the definition of the NP pressure index used in Trenberth and Hurrell (1994). Stippling indicates areas where the observed trends are within the simulated range of trends in the SMURPHS experiments, with the exception of Figures 3 and 8. In these latter figures, stippling is used to indicate areas where trends are statistically significant according to a two-sided Student's t-test at the 5% level. Annual means are shown in all figures except Figure 7, where trends over the October to March extended season are shown instead.

## 3. Results

### 3.1. Pacific Decadal Variability in CMIP6

In the period from 1981 until 2012, observed trends in surface temperatures show regions of warming and cooling in the Pacific and the Southern Ocean (Figure 2b), in a pattern that projects onto the negative phase of the PDO. During this period, most CMIP6 climate models simulate trends exceeding the observed rate of warming (Figure 2a), though there are realizations that simulate similar or lower rates of warming to those observed. The CMIP6 ensemble mean trend pattern shows spatially varying rates of warming, but importantly there are no areas of cooling. This lack of cooling suggests that any forced cooling (e.g., in response to anthropogenic aerosols) is outweighed by warming from greenhouse gases and natural forcings over this period in the multi-model average (Figures 2a and 2b). Indeed, the forced response to anthropogenic aerosols is relatively small over this time period and diverse across climate models (Figure 2a).

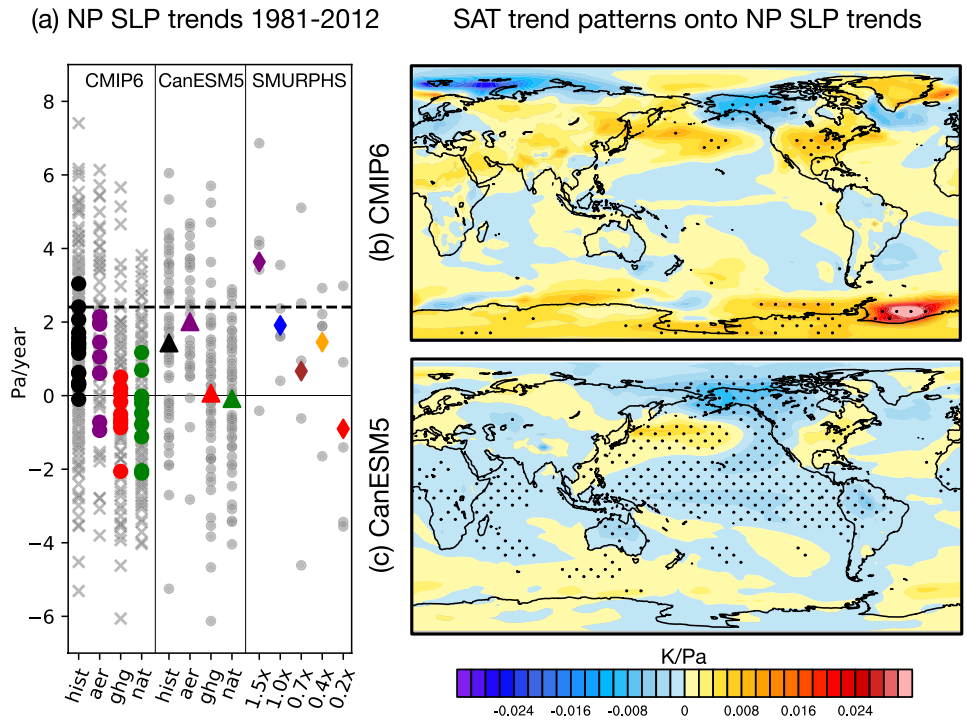


**Figure 3.** (a) Trends in annual mean North Pacific sea level pressure (measured by the NP index, Methods) in the CMIP6 historical, hist-aer, hist-GHG, and hist-nat experiments, respectively, for 1981–2012. Solid dots indicate ensemble means for each model with more than three ensemble members. The same is also shown for the CanESM5 large ensemble separately, as well as all of the SMURPHS scaled aerosol experiments. Ensemble means are shown by triangles and lozenges, respectively. The dashed line shows the observed trend from HadSLP2. (b) Pattern obtained from regressing historical ensemble mean 1981–2012 SAT trends for each of 14 CMIP6 models onto NP SLP trends from the same models, that is, the regression is across the ensemble dimension and one point in the regression represents one model. Only ensemble means from models with >= 3 ensemble members are used in the regression and all members available for a given variable are used to compute the model means. (c) The same regression of SAT trends onto NP SLP trends is shown for the 50 historical members of CanESM5. Stippling indicates statistical significance in a two-tailed t-test at the 5% level.

While aerosol forcing has been shown to be important in driving variations in surface temperatures in numerous studies, including in the SMURPHS ensemble (Dittus et al., 2020), the largest variations in GMST due to aerosol forcing are found in the period between around 1945 and 1975, when emissions increased rapidly across the globe. In the 1981–2012 period, global emissions of $SO_2$ are relatively constant, due to compensating trends between North America and Europe combined, where emissions have been decreasing since the late 1970s, and trends over Asia where emissions have continued to increase over this period (Figures 1a and 1b). Globally averaged, black and organic carbon emissions on the other hand have continued to increase during this time period. Consequently, model responses to aerosol over this period can be very different (Figure 2a), as different aerosol schemes are more or less sensitive to regional aerosol emissions. Additionally, internal variability may also explain some of the differences between models, as the residual internal variability in three-member ensemble means may still be quite large, especially in this period of relatively weak global aerosol forcing.

There are individual realizations in the CMIP6 ensemble that have a cooling pattern of Pacific SATs similar to those observed. Two individual ensemble members are shown in Figure 2b that look the most and the least like observations, based on pattern correlations over the Pacific, respectively. This is done to illustrate the range of patterns seen across CMIP6 only and is not indicative of model performance. However, members that have similar SAT patterns to observations are infrequent and, in most cases, the cooling is weaker than observed (not shown). This discrepancy could suggest a bias in the forced response or errors in the representation of internal variability in many CMIP6 models. However, it is also possible that the real world was in an unusual phase of internal variability during this time, and the models are consistent with observations when internal variability is considered (Olonscheck et al., 2020). In the following sections, the role of anthropogenic aerosols in driving this

cooling pattern in the Pacific is investigated by revisiting the question of whether anthropogenic aerosols played a role as a driver of a negative PDO.

The PDO has been widely studied and has previously been described as a superposition of various processes (Newman et al., 2016). One of the many drivers of North Pacific SSTs is sea level pressure in the North Pacific, in the region of the Aleutian Low. While other mechanisms may also be important and respond to aerosol forcing, the primary pathway that has been proposed for aerosols to affect the PDO is via changes in the Aleutian Low, so the remainder of the paper will focus on this mechanism.

In CMIP6, most models (14 out of 15 with >= 3 ensemble members) simulate increases in annual mean North Pacific sea level pressure in their historical simulations over the period from 1981 to 2012 (Figure 3a). Results from the DAMIP simulations suggest that this increase is primarily driven by increases in anthropogenic aerosols, as all but two models with more than three ensemble members simulate an increase in SLP during that period. In contrast, neither GHGs nor natural forcings can explain these trends in historical SLP (Figure 3a). It is unclear whether the two models showing a decrease in SLP in response to anthropogenic aerosols have a different forced response to anthropogenic aerosols to the other models or whether this is due to an insufficient number of ensemble members to isolate the forced response in NP SLP. Indeed, results from the CanESM5 large ensemble show that internal variability in NP SLP could be large and that more than three ensemble members may be needed to reliably determine the forced response. However, at the time of writing, only 5 models had more than three ensemble members available for the DAMIP simulations, so the 3-ensemble member threshold was chosen as a compromise between sampling internal variability and model diversity. Nevertheless, the majority of models do simulate an increase in NP SLP in response to anthropogenic aerosols.

Figures 3b and 3c show the pattern of surface air temperatures (SATs) associated with variations in the magnitude of trends in NP SLP across CMIP6 models and within the CanESM5 historical ensemble. Both CMIP6 and CanESM5 suggest that larger increases in NP SLP are associated with a negative PDO. For CMIP6, the temperature trend patterns from each of 14 CMIP6 models with at least three ensemble members are regressed onto the NP SLP trends from the same 14 models. Hence, the CMIP6 regression is also sensitive to differences in factors such as climate sensitivity in addition to internal variability assessed in CanESM5, which may account for its lower significance. Nevertheless, both patterns provide further evidence that NP SLP trends affect Pacific SAT trends.

In summary, Figure 3b shows that trends in NP SLP affect SAT trends in the Pacific across CMIP6 models, while Figure 3a shows that anthropogenic aerosol forcing can drive an increase in NP SLP. Together, these results suggest that changes in anthropogenic aerosol emissions in the period from 1981 to 2012 have contributed to Pacific variability in at least some CMIP6 models. However, it is not simply the case that models with the strongest aerosol forcing have the strongest response in SLP and Pacific SATs and vice-versa (not shown). Differences in model representation of aerosol and their processes combined with the limited number of ensemble members in the presence of large internal variability make it difficult to identify the reasons between the different responses across CMIP6 models and to provide a robust quantification of the fraction of Pacific variability driven by anthropogenic aerosols. Therefore, dedicated experiments to investigate the response to aerosol forcing in the presence of large internal variability are required to better understand the processes involved.

### 3.2. Mechanisms for a Response of North Pacific SATs to Anthropogenic Aerosols in the SMURPHS Ensemble

To investigate the mechanisms of a Pacific SAT response to anthropogenic aerosols further, we now focus on the SMURPHS ensemble of climate model simulations with HadGEM3-GC3.1, where anthropogenic aerosols have been scaled to sample a wide range of uncertainty in historical aerosol forcing (Dittus et al., 2020). Since the only difference between the experiments is the level of anthropogenic aerosol emissions, significant differences between the experiments can be directly attributed to differences in anthropogenic aerosol forcing.

Much like the CMIP6 multi-model mean, the five-member ensemble means for each aerosol-scaling experiment in the SMURPHS simulations show large-scale warming regardless of aerosol forcing, although there are also differences between the experiments (Figure 4). For example, the rate of warming is reduced in the high aerosol simulations, particularly in the polar regions and the eastern North Pacific. The 0.4, 0.7, 1.0, and 1.5 ensemble means show increasing areas of cooling in the South Pacific and the Southern Ocean, indicating that part of this

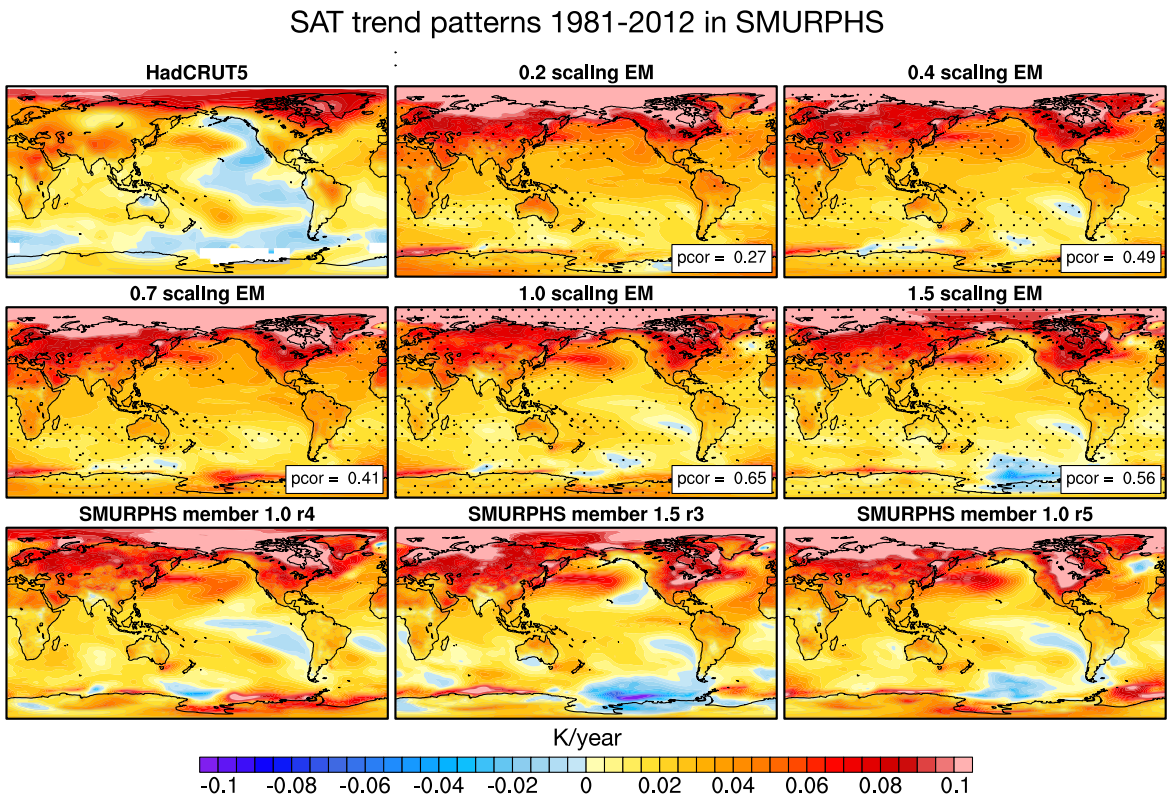


**Figure 4.** 1981–2012 annual mean surface temperature trends in HadCRUT5 and the five-member ensemble means of each of the SMURPHS scaled aerosol experiments (panels 1–6). Stippling is applied in regions where the observed trend lies within the range of simulated trends in the respective scaling ensemble. Pattern correlations calculated between the five-member ensemble mean trends and HadCRUT5 over the Pacific region are shown for all experiments. The surface temperature trends in the three realizations that have the highest pattern correlation with the observed SAT trends over the Pacific are shown for illustration purposes in panels 7–9. All pattern correlations were calculated between −50 to 50°N and 90 to 270°E.

SAT pattern may be externally forced, with differences between the experiments attributable to anthropogenic aerosols. The effect of increasing aerosol forcing across scaling experiments is clearer when the greenhouse gas-induced warming trend has been removed from all experiments in the SMURPHS ensemble (Figure 5). Overall, there are individual ensemble members in the SMURPHS ensemble that resemble the observed negative PDO pattern, but the cooling in those members is much weaker than observed in all cases. This is illustrated in Figure 4 by showing the three members with the highest pattern correlation in the Pacific. This is likely related to the finding that all ensemble members warm more rapidly than observations over this period (Dittus et al. (2020), also shown in Figure 2) and may be a feature common to other CMIP6 generation models (see Discussion). Nevertheless, the differences between the experiments suggest a role for anthropogenic aerosols in driving these SAT patterns, which we now examine further.

NP SLP trends are broadly larger with each higher aerosol scaling experiment, thus clearly demonstrating the sensitivity of North Pacific SLP to changes in aerosol over this period (Figures 3 and 6). Note that the trends in the 1.0 and 1.5 experiments are statistically significant at the 5% level and that the zonal winds at 250 hPa show changes consistent with these NP SLP trends (not shown). Observations from HadSLP2 over the same time period also show an increase in NP SLP, indicating that simulated aerosol-induced trends in SLP are consistent with observations over this time period. However, it is also important to note that Figure 6 shows 5-member ensemble means for the modeled trends, while the observations are by definition a single realization. While the higher aerosol simulated patterns appear more similar to observations than those from the low aerosol experiments, due to the large contribution from internal variability trends such as those seen in observations could also arise from internal variability and occur in individual realizations in some of the lower aerosol experiments (Figure 3a). Substantial internal variability across ensemble members can also be seen in the time series of 20-year running means in NP SLP (Figure 6b). Additionally, these time series also show that there is substantial low-frequency

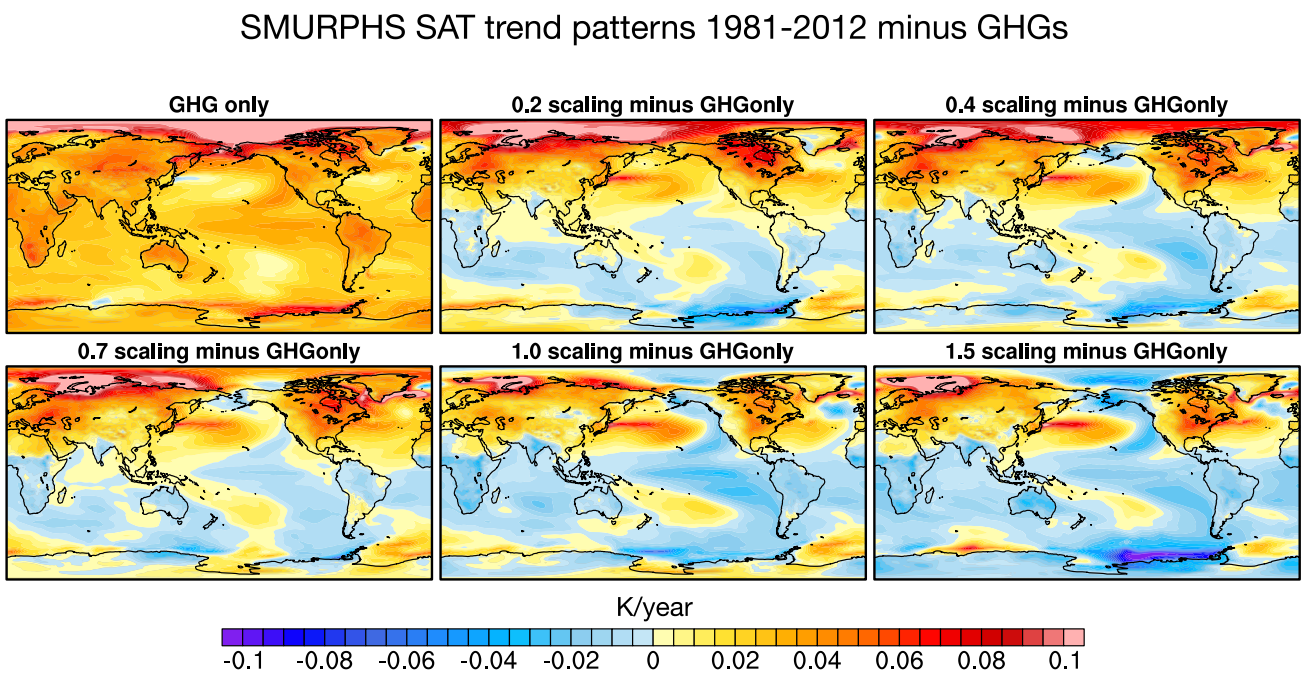


**Figure 5.** Annual mean surface temperature trends in the greenhouse gas (GHG) only DAMIP experiment for HadGEM3-GC3.1-LL (four member ensemble mean) and surface temperature trends in the SMURPHS experiments, where the GHG-only pattern from the DAMIP experiments has been removed.

variability in these time series, likely due to different forcings in different time periods, including but not limited to aerosols and greenhouse gases. The end of these time series also shows the sensitivity of NP SLP to anthropogenic aerosol forcing since the 1980s shown in Figures 3 and 6a, with NP SLP decreasing in the low aerosol simulations and increasing in the higher aerosol simulations.

Meridional wind trends at 250 hPa show a pattern of alternating positive and negative wind anomalies emerging in the higher aerosol scaling experiments (Figure 7). These patterns suggest that a Rossby Wave train across the Pacific may be being triggered in the higher aerosol simulations, consistent with previous studies that showed a Rossby Wave response to changes in Asian aerosol emissions (Smith et al., 2016; Wilcox et al., 2019). A similar pattern in meridional wind trends is seen in the ERA5 reanalysis over the Pacific in the same time period (Figure 7), but the trends in ERA5 are much stronger. Since this is predominately a winter signal, the extended winter season is shown in Figure 7. With only one realization of the real historical climate, it is not possible to say whether the stronger trends in ERA5 are due to an underestimation of the forced response in climate models or simply due to a particular realization of internal variability in the real world.

The information shown in Figures 5–7 is summarized in Figure 8 and compared to earlier time periods. Figure 8 shows the regression of temperature (left), SLP (middle) and meridional winds (right) trend patterns from each realization onto the absolute value of the 2014 aerosol effective radiative forcing for each experiment (−0.38, −0.60, −0.93, −1.17, and −1.50 W/m$^2$). In other words, it shows how the trend patterns change as a function of strengthening aerosol forcing across all 25 ensemble members of the SMURPHS ensemble. Figure 8 shows the patterns associated with an increase in anthropogenic aerosol forcing for each variable in each time period, in the absence of responses to other forcings (since these are identical across all experiments, they do not influence the regression).

As expected, a stronger aerosol forcing is associated with a larger relative decrease in global temperatures in all time periods. The strongest cooling occurs in the period from 1951 to 1980, corresponding to the period where changes in global aerosol burden are largest across the ensemble, while the changes are weakest in the period from 1921 to 1950. Importantly, however, this figure highlights that the responses to anthropogenic aerosol forcing during the 1981–2012 period differ from earlier periods. In particular, it is the period with the strongest (and most significant) atmospheric circulation responses to anthropogenic aerosol over the Pacific, while the

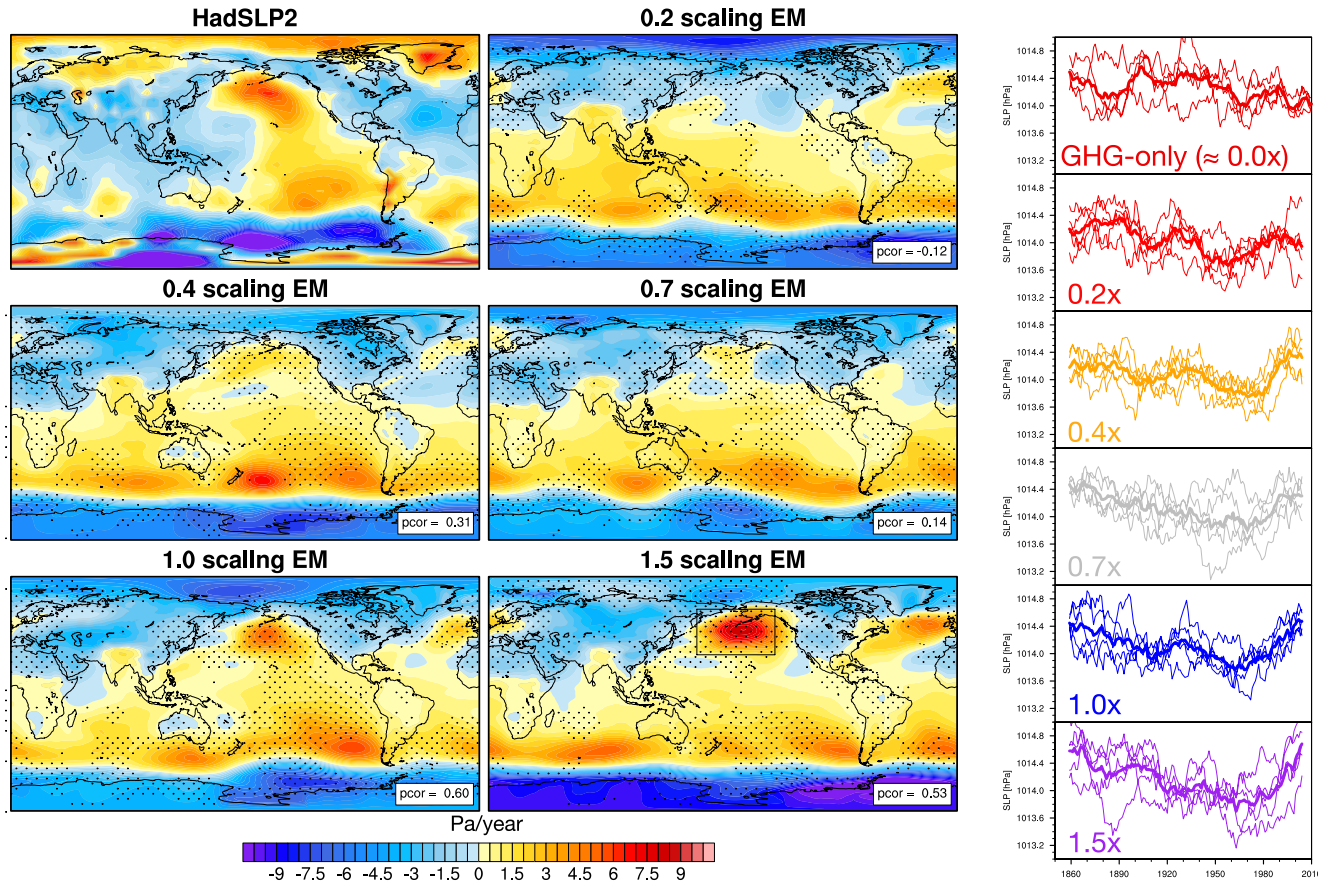


**Figure 6.** 1981–2012 annual mean sea level pressure trends for HadSLP2 and each of the five-member ensemble means across scalings. Stippling is applied in regions where the observed trend lies within the range of simulated trends in the respective scaling ensemble. Pattern correlations calculated between the five-member ensemble mean trends and HadSLP2 are shown for all experiments. The pattern correlations were calculated between −50 to 50°N and 90 to 270°E. The 20-year running-mean time series for the NP box (black box in panel 6 and Methods) are shown on the right for all scalings and the GHG-only simulations (approx. 0.0 scaling).

preceding periods are dominated by global cooling but seemingly weaker circulation responses. As the globally averaged aerosol forcing over the most recent time period is approximately constant, it is likely the regional changes in aerosol emissions that are important in explaining the changes over 1981–2012. Indeed, while European and North American aerosol emissions have been declining over this period, Asian emissions have been at their highest levels and with the most rapid growth since 1850 (Figure 1), suggesting that Asian aerosol emissions are a plausible driver of the changes seen in this period. This hypothesis is consistent with results from a previous study that has shown a Rossby-Wave response with a similar structure to increases in Asian aerosol emissions over the same time period in a predecessor of this model, HadGEM3-GC2 (Wilcox et al., 2019). Furthermore, the 1981–2012 period is also the period with the strongest black carbon emission increases (Figure 1). A recent study has suggested that the increase in NP SLP is primarily a response to black carbon aerosols rather than sulfate aerosols (Dow et al., 2021), but we do not differentiate between different species of anthropogenic aerosols here.

## 4. Discussion and Broader Implications

The results presented in this paper provide further evidence that anthropogenic aerosols likely contributed to driving variations in North Pacific SATs since the 1980s in at least some CMIP6 models. This is associated with an increase in NP SLP and, in HadGEM3, a Rossby Wave train across the Pacific. Consistency of the response pattern shown here with previous studies suggests that the response is likely to be driven by changes in Asian aerosol emissions, which induce local circulation changes and initiate a Rossby wave train from the midlatitudes as shown in Smith et al. (2016) and Wilcox et al. (2019). Assessment of the role of different aerosol species by Dow et al. (2021) suggests an important role for black carbon emissions over Asia in particular, with emissions from

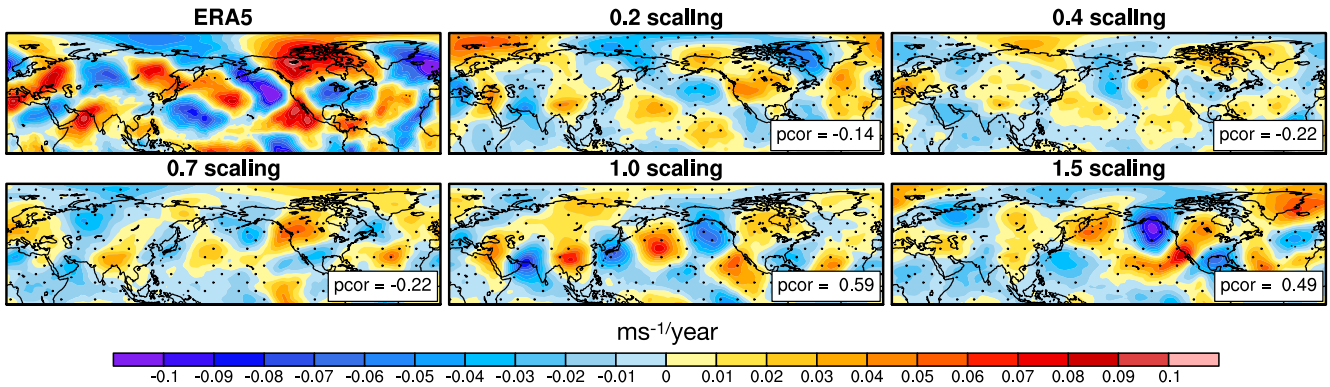


**Figure 7.** 1981–2012 extended boreal winter season trends (ONDJFM) in meridional winds at 250 hPa in the SMURPHS experiments (five-member ensemble means shown) and the ERA5 reanalysis. Stippling is applied in regions where the observed trend lies within the range of simulated trends in the respective scaling ensemble. Pattern correlations calculated between the five-member ensemble mean trends and ERA5 are shown for all experiments. The pattern correlations were calculated between −10 to 50°N and 90 to 270°E.

elsewhere enhancing the response. It is possible that other pathways exist by which anthropogenic aerosols could affect Pacific Decadal Variability. For example, studies have shown that Atlantic temperature trends can affect SATs in the tropical Pacific (McGregor et al., 2014). It has separately been suggested that Atlantic Multi-decadal Variability could be influenced by anthropogenic aerosols (Booth et al., 2012), though research into that topic is ongoing (e.g., Andrews et al., 2020; Kim et al., 2018; Zhang et al., 2013). It is therefore plausible that other

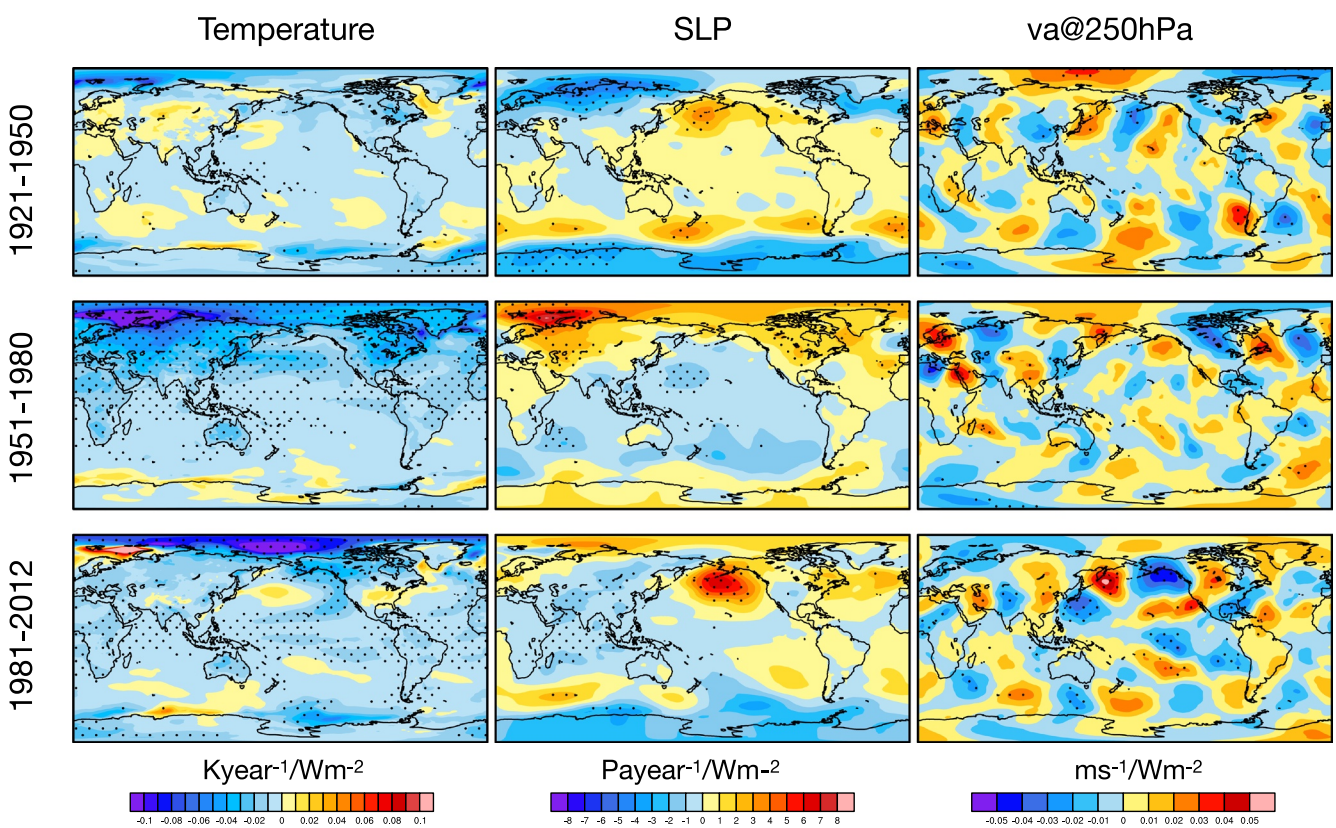


**Figure 8.** Regression of 30-year trends (32 years for the most recent period) across present-day aerosol forcing strength (2014 aerosol ERF) across SMURPHS ensemble for temperature, pressure, and meridional winds at 250 hPa, respectively. Sign convention is such that the pattern corresponds to the pattern associated with an increase in aerosol forcing (i.e., a negative forcing becoming more negative). Stippling indicates statistical significance in a two-tailed t-test at the 5% level.

pathways exist in which anthropogenic aerosols could influence Pacific Decadal Variability, but further analysis of these is left for future studies.

A key uncertainty in interpreting these results is how simulated Pacific Decadal Variability relates to real-world Pacific Decadal Variability. Indeed, several previous studies have identified issues in how the previous generation of climate models represent tropical Pacific variability, with suggestions that models underestimate variability at multi-decadal scales and longer (e.g., Ault et al., 2013; Capotondi et al., 2015; Kajtar et al., 2019). In addition, difficulties in capturing ENSO characteristics accurately and biases in the connection between the Atlantic and Pacific basins mean that it is difficult to quantify the fraction of the observed trends that is attributable to anthropogenic aerosols (e.g., Capotondi et al., 2015; Deser et al., 2018; McGregor et al., 2018; Zhao et al., 2021; Power et al., 2021 and references therein). These issues, among others, likely contribute to the apparent discrepancy between observed and simulated Pacific SAT trend patterns over this time period. Although there are some ensemble members across CMIP6 that appear to be able to simulate patterns that resemble the SAT pattern seen in observations, these patterns are, on average, much weaker than observed. Only very few ensemble members in all of CMIP6 show a basin-wide cooling as strong as the one seen in observations.

One possible contributing factor to explain this difference is that climate models may underestimate the atmospheric circulation responses to external forcing (Scaife & Smith, 2018), potentially related to an underestimation of the eddy feedback (Scaife et al., 2019). A recent study has shown that the predictable signal for the North Atlantic Oscillation is underestimated in climate models by an order of magnitude (Smith et al., 2020). It is plausible that this may also be the case for the response of other aspects of the atmospheric circulation to external forcing, and by extension, affect the response of the North Pacific climate system to aerosol forcing. If this were the case, it is possible the circulation-mediated temperature response to aerosol forcing seen in the models may be too weak.

However, this is only one of several hypotheses that have been proposed in the literature to explain the difference between observed and simulated temperature trends during this period, both in the Pacific and globally. It is well documented that the Pacific plays an important role in setting the rate of GMST warming. The remaining hypotheses to reconcile observed and simulated temperature trends broadly fall into the following categories: current GCMs are too sensitive to greenhouse-gas forcing (Dittus et al., 2020; Nijsse et al., 2020; Tokarska et al., 2020) and/or have errors in the forced response (Seager et al., 2019); Pacific cooling is underestimated due to an incorrect response to volcanic eruptions (Gregory et al., 2019); the simulated internal variability is too weak (Capotondi et al., 2015; Gregory et al., 2019), or the real-world was experiencing a really unusual phase of internal variability during this time and the models are in fact consistent with observations (Olonscheck et al., 2020). We refer the reader to the papers cited above for more discussion of these possible causes and suggest that further research is needed to better understand this issue.

Recent papers have argued that climate projections from high climate sensitivity models are unrealistic, as the rapid warming seen in those models is inconsistent with recent historical trends (Brunner et al., 2020). Studies have also suggested that the transient climate response (TCR) to greenhouse gases is unrealistically high by using the period since the 1980s to constrain the transient climate response (Dittus et al., 2020; Nijsse et al., 2020; Tokarska et al., 2020). These conclusions rely on the assumption that internal variability and the responses to anthropogenic aerosols and volcanoes are all simulated realistically over this period. Therefore, it is imperative that future work address this question, as the interpretation of projections from high sensitivity models relies upon knowing which of the above hypotheses is correct. Regardless of the cause of the observed negative PDO in the real world, a reversal of this trend would be expected to lead to enhanced near-term warming, potentially amplified by cloud and lapse-rate feedbacks becoming more positive (Andrews & Webb, 2018).

## 5. Conclusions

We analyze large multi-model ensembles of CMIP6 historical and DAMIP simulations, together with the SMURPHS ensemble of scaled aerosol-forcing experiments (Dittus et al., 2020). We provide robust evidence that anthropogenic aerosols likely contributed to an increase in North Pacific (NP) SLP over the period from 1981 to 2012 in multiple climate models, in agreement with previous analysis of CMIP5 simulations (Oudar et al., 2018; Smith et al., 2016). The SMURPHS ensemble provides an opportunity to assess the physical processes in more detail by correlating the forced response with the strength of the aerosol forcing. This analysis

reveals a meridional wind anomaly pattern in response to stronger aerosol emissions that is consistent with a Rossby wave train over the North Pacific. These results are consistent with previous studies that showed a Rossby wave response to Asian aerosol emissions since the 1980s (Wilcox et al., 2019) and aerosol-forced changes in Rossby wave source in the north-west Pacific (Smith et al., 2016). A similar pattern of meridional wind anomalies resembling a Rossby wave train, along with an increase in NP SLP, is also seen in reanalysis and observations, respectively, suggesting that anthropogenic aerosols may have plausibly played a role in driving real-world changes over this period.

NP SLP can influence the PDO (Newman et al., 2016) and has previously been proposed as a possible mechanism through which anthropogenic aerosol can affect its phase (Smith et al., 2016). We provide two new lines of evidence that support this connection over the period 1981 to 2012. First, in the CMIP6 simulations stronger aerosol-forced trends in NP SLP are associated with a more negative PDO. Second, regressing across the SMURPHS ensemble shows that increased aerosol forcing projects onto the negative phase of the PDO. However, this aerosol-forced negative PDO pattern is overwhelmed by warming from greenhouse gases in the CMIP6 and SMURPHS simulations such that their ensemble means show little resemblance to the observations, and the majority of model simulations overestimate the observed GMST trends.

The reason for differences between model simulations and observations over the 1981–2012 period remains open. It is possible that unusually strong internal variability coincidentally aligned with the aerosol-forced response in the real world and that models are consistent with observations, even if the observations lie toward one end of the distribution. However, errors in the simulated characteristics of internal variability in the Pacific and/or biases in either the response to greenhouse gases, the response to volcanic eruptions or the circulation-mediated response to anthropogenic aerosols in current climate models are also plausible sources of differences between models and observations. Given the role of atmospheric circulation in the aerosol-forced negative PDO, the latter would be consistent with evidence from seasonal and decadal predictions that models underestimate atmospheric circulation changes (Scaife & Smith, 2018; Smith et al., 2020). Of course, it is possible (and perhaps even likely) that a combination of these may be applicable. Which of these hypotheses are correct has important implications for whether climate projections from high climate sensitivity models are considered plausible or not, and it is, therefore, crucial that future research addresses these questions.

## Data Availability Statement

Output from the SMURPHS climate model ensemble is archived at the Centre for Environmental Data Analysis https://catalogue.ceda.ac.uk/uuid/5808b237bdb5485d9bc3595f39ce85e3. CMIP6 data can be accessed via the Earth System Grid Federation.

**Acknowledgments**
The authors gratefully acknowledge support from the DOVE project as part of the UK–China Research and Innovation Partnership Fund through the Met Office Climate Science for Service Partnership (CSSP) China as part of the Newton Fund. A. J. Dittus was supported by the Natural Environment Research Council (SMURPHS project, grant NE/N006054/1) and the DOVE project. E. H. Hawkins, J. I. Robson, and L. J. Wilcox were supported by the National Centre for Atmospheric Science. DMS was supported by the Met Office Hadley Centre Climate Programme funded by BEIS and Defra and by the European Commission Horizon 2020 CONSTRAIN project (GA 820829). We acknowledge use of the Monsoon2 system, a collaborative facility supplied under the Joint Weather and Climate Research Programme, a strategic partnership between the Met Office and the Natural Environment Research Council. We acknowledge the World Climate Research Programme, which through its Working Group on Coupled Modelling, coordinated and promoted CMIP6. We thank the climate modeling groups for producing and making available their model output, the Earth System Grid Federation (ESGF) for archiving the data and providing access, and the multiple funding agencies who support CMIP6 and ESGF. Hersbach et al., (2019) was downloaded from the Copernicus Climate Change Service (C3S) Climate Data Store. The results contain modified Copernicus Climate Change Service information 2020. Neither the European Commission nor ECMWF is responsible for any use that may be made of the Copernicus information or data it contains. The authors would like to thank Prof. Rowan Sutton, Prof. Jonathan Gregory, Dr. Richard Wood, Dr. Giorgio Graffino, Dr. Dan Hodson, and Dr. Ben Booth for useful discussions and two anonymous reviewers for constructive comments on the paper that helped improve the manuscript.

## References

Allan, R., & Ansell, T. (2006). A New Globally Complete Monthly Historical Gridded Mean Sea Level Pressure Dataset (HadSLP2): 1850–2004. *Journal of Climate*, *19*(22), 5816–5842. https://doi.org/10.1175/jcli3937.110.1175/jcli3937.1

Andrews, M. B., Ridley, J. K., Wood, R. A., Andrews, T., Blockley, E. W., Booth, B., et al. (2020). Historical simulations with HadGEM3-GC3.1 for CMIP6. *Journal of Advances in Modeling Earth Systems*, *12*, e2019MS001995. https://doi.org/10.1029/2019MS001995

Andrews, T., & Webb, M. J. (2018). The dependence of global cloud and lapse rate feedbacks on the spatial structure of tropical pacific warming. *Journal of Climate*, *31*(2), 641–6541. https://doi.org/10.1175/jcli-d-17-0087.1

Ault, T. R., Deser, C., Newman, M., & Emile-Geay, J. (2013). Characterizing decadal to centennial variability in the equatorial Pacific during the last millennium. *Geophysical Research Letters*, *40*, 3450–3456. https://doi.org/10.1002/grl.50647

Barnett, T. P., Pierce, D. W., Latif, M., Dommenget, D., & Saravanan, R. (1999). Inter-decadal interactions between the tropics and midlatitudes in the Pacific Basin. *Geophysical Research Letters*, *26*(5), 615–618. https://doi.org/10.1029/1999gl900042

Bellouin, N., Quaas, J., Gryspeerdt, E., Kinne, S., Stier, P., Watson-Parris, D., et al. (2020). Bounding global aerosol radiative forcing of climate change. *Reviews of Geophysics*, *58*(1). https://doi.org/10.1029/2019rg000660

Boo, K.-O., Booth, B. B. B., Byun, Y.-H., Lee, J., Cho, C., Shim, S., & Kim, K.-T. (2015). Influence of aerosols in multidecadal SST variability simulations over the North Pacific. *Journal of Geophysical Research: Atmosphere*, *120*, 517–531. https://doi.org/10.1002/2014jd021933

Booth, B. B. B., Dunstone, N. J., Halloran, P. R., Andrews, T., & Bellouin, N. (2012). Aerosols implicated as a prime driver of twentieth-century North Atlantic climate variability. *Nature*, *484*(7393), 228–232. https://doi.org/10.1038/nature10946

Brunner, L., Pendergrass, A. G., Lehner, F., Merrifield, A. L., Lorenz, R., & Knutti, R. (2020). Reduced global warming from CMIP6 projections when weighting models by performance and independence. *Earth System Dynamics*, *11*(4), 995–1012. https://doi.org/10.5194/esd-11-995-2020

Capotondi, A., Wittenberg, A. T., Newman, M., Di Lorenzo, E., Yu, J., Braconnot, P., et al. (2015). Understanding ENSO Diversity. *Bulletin of the American Meteorological Society*, *96*(6), 921–938. https://doi.org/10.1175/bams-d-13-00117.1

Deser, C., Phillips, A. S., Simpson, I. R., Rosenbloom, N., Coleman, D., Lehner, F., et al. (2020). Isolating the evolving contributions of anthropogenic aerosols and greenhouse gases: A new CESM1 large ensemble community resource. *Journal of Climate*, *33*(18), 7835–7858. https://doi.org/10.1175/jcli-d-20-0123.1

Deser, C., Simpson, I. R., Phillips, A. S., & McKinnon, K. A. (2018). How well do we know ENSO's climate impacts over North America and how do we evaluate models accordingly? *Journal of Climate*, *31*, 4991–5014. American Meteorological Society. https://doi.org/10.1175/jcli-d-17-0783.1

Dittus, A. J., Hawkins, E., Wilcox, L. J., Sutton, R. T., Smith, C. J., Andrews, M. B., & Forster, P. M. (2020). Sensitivity of historical climate simulations to uncertain aerosol forcing. *Geophysical Research Letters*, *47*(13). https://doi.org/10.1029/2019gl085806

Dong, B., & Dai, A. (2015). The influence of the Interdecadal Pacific Oscillation on temperature and precipitation over the globe. *Climate Dynamics*, *45*(9–10), 2667–2681. https://doi.org/10.1007/s00382-015-2500-x

Dow, W. J., Maycock, A. C., Lofverstrom, M., & Smith, C. J. (2021). The effect of anthropogenic aerosols on the Aleutian low. *Journal of Climate*, *34*(5), 1725–1741. https://doi.org/10.1175/jcli-d-20-0423.1

England, M. H., McGregor, S., Spence, P., Meehl, G. A., Timmermann, A., Cai, W., et al. (2014). Recent intensification of wind-driven circulation in the Pacific and the ongoing warming hiatus. *Nature Climate Change*, *4*(3), 222–227. https://doi.org/10.1038/nclimate210610.1038/nclimate2106

Eyring, V., Bony, S., Meehl, G. A., Senior, C. A., Stevens, B., Stouffer, R. J., & Taylor, K. E. (2016). Overview of the Coupled Model Intercomparison Project Phase 6 (CMIP6) experimental design and organization. *Geoscientific Model Development*, *9*(5), 1937–1958. https://doi.org/10.5194/gmd-9-1937-2016

Gillett, N. P., Shiogama, H., Funke, B., Hegerl, G., Knutti, R., Matthes, K., et al. (2016). The Detection and Attribution Model Intercomparison Project (DAMIP v1.0) contribution to CMIP6. *Geoscientific Model Development*, *9*(10), 3685–3697. https://doi.org/10.5194/gmd-9-3685-2016

Gregory, J. M., Andrews, T., Ceppi, P., Mauritsen, T., & Webb, M. J. (2019). How accurately can the climate sensitivity to $$\\hbox {CO} {2}$$ be estimated from historical climate change? *Climate Dynamics*, *54*(1–2), 129–157. https://doi.org/10.1007/s00382-019-04991-y10.1007/s00382-019-04991-y

Hardiman, S. C., Andrews, M. B., Andrews, T., Bushell, A. C., Dunstone, N. J., Dyson, H., et al. (2019). The impact of prescribed ozone in climate projections run with HadGEM3-GC3.1. *Journal of Advances in Modeling Earth Systems*, *11*(11), 3443–3453. https://doi.org/10.1029/2019ms001714

Hersbach, H., Bell, B., Berrisford, P., Biavati, G., Horányi, A., Muñoz Sabater, J., et al. (2019). *ERA5 monthly averaged data on pressure levels from 1979 to present*. https://doi.org/10.24381/cds.6860a573ere

Kajtar, J. B., Collins, M., Frankcombe, L. M., England, M. H., Osborn, T. J., & Juniper, M. (2019). Global mean surface temperature response to large-scale patterns of variability in observations and CMIP5. *Geophysical Research Letters*, *46*(4), 2232–2241. https://doi.org/10.1029/2018gl081462

Kim, W. M., Yeager, S. G., & Danabasoglu, G. (2018d). Key role of internal ocean dynamics in atlantic multidecadal variability during the last half century. *Geophysical Research Letters*, *45*(24). https://doi.org/10.1029/2018gl080474

Kosaka, Y., & Xie, S.-P. (2013). Recent global-warming hiatus tied to equatorial Pacific surface cooling. *Nature*, *501*(7467), 403–407. https://doi.org/10.1038/nature12534

Liguori, G., McGregor, S., Arblaster, J. M., Singh, M. S., & Meehl, G. A. (2020j). A joint role for forced and internally-driven variability in the decadal modulation of global warming. *Nature Communications*, *11*(1). https://doi.org/10.1038/s41467-020-17683-7

Maher, N., Gupta, A. S., & England, M. H. (2014). Drivers of decadal hiatus periods in the 20th and 21st centuries. *Geophysical Research Letters*, *41*(16), 5978–5986. Retrieved from https://doi.org/10.1002/2014gl060527

Mantua, N. J., & Hare, S. R. (2002). The Pacific decadal oscillation. *Journal of Oceanography*, *58*(1), 35–44. https://doi.org/10.1023/a:1015820616384

McGregor, S., Stuecker, M. F., Kajtar, J. B., England, M. H., & Collins, M. (2018). Model tropical Atlantic biases underpin diminished Pacific decadal variability. *Nature Climate Change*, *8*(6), 493–498. https://doi.org/10.1038/s41558-018-0163-4

McGregor, S., Timmermann, A., Stuecker, M. F., England, M. H., Merrifield, M., Jin, F.-F., & Chikamoto, Y. (2014). Recent Walker circulation strengthening and Pacific cooling amplified by Atlantic warming. *Nature Climate Change*, *4*(10), 888–892. https://doi.org/10.1038/nclimate2330

McPhaden, M. J., Zebiak, S. E., & Glantz, M. H. (2006). ENSO as an integrating concept in Earth Science. *Science*, *314*(5806), 1740–1745. https://doi.org/10.1126/science.1132588

Medhaug, I., Stolpe, M. B., Fischer, E. M., & Knutti, R. (2017). Reconciling controversies about the 'global warming hiatus. *Nature*, *545*(7652), 41–47. https://doi.org/10.1038/nature22315

Meehl, G. A., Hu, A., Arblaster, J. M., Fasullo, J., & Trenberth, K. E. (2013). Externally forced and internally generated decadal climate variability associated with the interdecadal Pacific oscillation. *Journal of Climate*, *26*(18), 7298–7310. https://doi.org/10.1175/jcli-d-12-00548.1

Meehl, G. A., Hu, A., Santer, B. D., & Xie, S.-P. (2016). Contribution of the interdecadal Pacific oscillation to twentieth-century global surface temperature trends. *Nature Climate Change*, *6*(11), 1005–1008. https://doi.org/10.1038/nclimate3107

Morice, C. P., Kennedy, J. J., Rayner, N. A., Winn, J. P., Hogan, E., Killick, R. E., et al. (2021). An updated assessment of near-surface temperature change from 1850: The HadCRUT5 Data Set. *Journal of Geophysical Research: Atmosphere*, *126*(3). https://doi.org/10.1029/2019jd032361

Newman, M., Alexander, M. A., Ault, T. R., Cobb, K. M., Deser, C., Lorenzo, E. D., et al. (2016). The Pacific decadal oscillation revisited. *Journal of Climate*, *29*(12), 4399–44271. https://doi.org/10.1175/jcli-d-15-0508.1

Nijsse, F. J. M. M., Cox, P. M., & Williamson, M. S. (2020). *An emergent constraint on transient warming from simulated historical warming in CMIP6 models*. https://doi.org/10.5194/egusphere-egu2020-19747

Olonscheck, D., Rugenstein, M., & Marotzke, J. (2020). Broad consistency between observed and simulated trends in sea surface temperature patterns. *Geophysical Research Letters*, *47*(10). https://doi.org/10.1029/2019gl086773

Oudar, T., Kushner, P. J., Fyfe, J. C., & Sigmond, M. (2018). No impact of anthropogenic aerosols on early 21st century global temperature trends in a large initial-condition ensemble. *Geophysical Research Letters*, *45*(17), 9245–9252. https://doi.org/10.1029/2018gl078841

Power, S., Casey, T., Folland, C., Colman, A., & Mehta, V. (1999). Inter-decadal modulation of the impact of ENSO on Australia. *Climate Dynamics*, *15*(5), 319–324. https://doi.org/10.1007/s003820050284

Power, S., Coauthors, M., Capotondi, A., Khodri, M., Vialard, J., Jebri, B., et al. (2021). Decadal climate variability in the tropical Pacific: Characteristics, causes, predictability, and prospects. *Science*, *374*, eaay9165. https://doi.org/10.1126/science.aay9165

Qin, M., Dai, A., & Hua, W. (2020). Aerosol-forced multidecadal variations across all ocean basins in models and observations since 1920. *Science Advances*, *6*(29), eabb0425. https://doi.org/10.1126/sciadv.abb0425

Salinger, M., Renwick, J., & Mullan, A. (2001). Interdecadal Pacific oscillation and South Pacific climate. *International Journal of Climatology*, *21*(14), 1705–1721. https://doi.org/10.1002/joc.691

Scaife, A. A., Camp, J., Comer, R., Davis, P., Dunstone, N., Gordon, M., et al. (2019). Does increased atmospheric resolution improve seasonal climate predictions? *Atmospheric Science Letters*, *20* (8). https://doi.org/10.1002/asl.922

Scaife, A. A., & Smith, D. (2018). A signal-to-noise paradox in climate science. *NPJ Climate and Atmospheric Science*, *1* (1). https://doi.org/10.1038/s41612-018-0038-4

Schneider, N., & Cornuelle, B. D. (2005). The forcing of the Pacific decadal oscillation. *Journal of Climate*, *18*(21), 4355–4373. https://doi.org/10.1175/jcli3527.1

Seager, R., Cane, M., Henderson, N., Lee, D.-E., Abernathey, R., & Zhang, H. (2019). Strengthening tropical Pacific zonal sea surface temperature gradient consistent with rising greenhouse gases. *Nature Climate Change*, *9* (7), 517–522. https://doi.org/10.1038/s41558-019-0505-x

Smith, D. M., Booth, B. B. B., Dunstone, N. J., Eade, R., Hermanson, L., Jones, G. S., et al. (2016). Role of volcanic and anthropogenic aerosols in the recent global surface warming slowdown. *Nature Climate Change*, *6*(10), 936–940. https://doi.org/10.1038/nclimate3058

Smith, D. M., Scaife, A. A., Eade, R., Athanasiadis, P., Bellucci, A., Bethke, I., et al. (2020). North Atlantic climate far more predictable than models imply. *Nature*, *583*(7818), 796–800. https://doi.org/10.1038/s41586-020-2525-0

Stolpe, M. B., Cowtan, K., Medhaug, I., & Knutti, R. (2020). Pacific variability reconciles observed and modelled global mean temperature increase since 1950. *Climate Dynamics*, *56*(1–2), 613–634. https://doi.org/10.1007/s00382-020-05493-y

Swart, N. C., Cole, J. N. S., Kharin, V. V., Lazare, M., Scinocca, J. F., Gillett, N. P., et al. (2019). The Canadian Earth System Model version 5 (CanESM5.0.3). *Geoscientific Model Development*, *12* (11), 4823–4873. https://doi.org/10.5194/gmd-12-4823-2019

Tokarska, K. B., Stolpe, M. B., Sippel, S., Fischer, E. M., Smith, C. J., Lehner, F., & Knutti, R. (2020). Past warming trend constrains future warming in CMIP6 models. *Science Advances*, *561*(12), eaaz9549. https://doi.org/10.1126/sciadv.aaz9549

Trenberth, K. E., & Hurrell, J. W. (1994). Decadal atmosphere-ocean variations in the Pacific. *Climate Dynamics*, *9* (6), 303–319. https://doi.org/10.1007/bf00204745

Wang, L., Chen, W., & Huang, R. (2008). Interdecadal modulation of PDO on the impact of ENSO on the East Asian winter monsoon. *Geophysical Research Letters*, *35*(20). https://doi.org/10.1029/2008gl035287

Wilcox, L. J., Dunstone, N., Lewinschal, A., Bollasina, M., Ekman, A. M. L., & Highwood, E. J. (2019). Mechanisms for a remote response to Asian anthropogenic aerosol in boreal winter. *Atmospheric Chemistry and Physics*, *19* (14), 9081–9095. https://doi.org/10.5194/acp-19-9081-2019

Wilcox, L. J., Highwood, E. J., Booth, B. B. B., & Carslaw, K. S. (2015). Quantifying sources of inter-model diversity in the cloud albedo effect. *Geophysical Research Letters*, *42*(5), 1568–1575. https://doi.org/10.1002/2015gl063301

Xie, S.-P., & Kosaka, Y. (2017). What caused the global surface warming Hiatus of 1998–2013? *Current Climate Change Reports*, *3*(2), 128–140. https://doi.org/10.1007/s40641-017-0063-0

Zanchettin, D., Franks, S. W., Traverso, P., & Tomasino, M. (2008). On ENSO impacts on European wintertime rainfalls and their modulation by the NAO and the Pacific multi-decadal variability described through the PDO index. *International Journal of Climatology*, *28*(8), 995–1006. https://doi.org/10.1002/joc.1601

Zhang, R., Delworth, T. L., Sutton, R., Hodson, D. L. R., Dixon, K. W., Held, I. M., et al. (2013). Have aerosols caused the observed Atlantic multidecadal variability? *Journal of the Atmospheric Sciences*, *70*(4), 1135–1144. https://doi.org/10.1175/jas-d-12-0331.1

Zhao, Y., Di Lorenzo, E., Sun, D., & Stevenson, S. (2021). Tropical Pacific decadal variability and ENSO precursor in CMIP5 Models, *Journal of Climate*, *34*(3), 1023–1045. https://doi.org/10.1175/jcli-d-20-0158.1